Spectroscopy 18 (2004) 503–511
IOS Press

Subcellular localisation of cholesterol and phosphocholine with pattern-recognition-imaging-TOF-SIMS

Per Malmberg [a], Håkan Nygren [a,*], Peter Sjövall [b] and Jukka Lausmaa [b]
[a] *Department of Anatomy and Cell Biology, Göteborg University, Göteborg, Sweden*
[b] *Department of Chemistry and Materials Technology, SP Swedish National Testing and Research Institute, Borås, Sweden*

Abstract. Molecular ions of cholesterol, and its fragments, and phosphocholine fragments of phospholipids, were localized in single cells with a resolution of <1 μm. This is the first example of subcellular localisation of membrane lipids with pattern-recognition, imaging time-of-flight secondary ion mass spectrometry (PRITS) here utilized for identification and subcellular localisation of cholesterol and phosphocholine in PMN leukocytes. Cell imprints were produced by transferring the cell constituents of freeze-dried cells to a silver foil, and the silver surface was analyzed by TOF-SIMS. TOF-SIMS spectra were recorded by scanning the primary ion beam over the analysis area and acquiring a positive mass spectrum of the ions leaving the surface. Data were collected at either high mass resolution $m/\Delta m > 7000$ or high lateral resolution. High mass resolution spectra were recorded on reference samples of pure cholesterol and phosphatidylcholine. Characteristic fragment peaks and the silver cationised quasimolecular ion $[M+Ag]^+$ were selected as a pattern for the identification of the lipids in TOF-SIMS images of surface-adhering leukocytes. The localisation of membrane lipids showed lateral heterogeneity over the cell surface.

1. Introduction

Information about the spatial distribution of molecules in cells is of general interest in cell biology and histology. The ability to localise and characterise plasma membrane lipids, for example in the study of lipid rafts and cellular signalling processes, is one important application. However, imaging of the chemical composition of biological samples at the subcellular level constitutes a major experimental challenge, and a general method for identification and localisation of biomolecules in cells is still lacking. Secondary ion mass spectrometry (SIMS) is a promising technique in this context and has been used for imaging the distribution of elements, chemically labelled biomolecules, and a limited number of specific organic molecules within cells [1–8]. However, extensive molecular characterisation of the cells has been hindered for several reasons, e.g., lack of sufficient ion yields and suitable sample handling methods [2]. A natural choice of sample handling, e.g., freeze drying has been reported not to be successful [1], whereas frozen hydrated freeze fractured biological samples have been used with some success [1,3], although the resulting TOF-SIMS images contained limited chemical information specific to the cells. With the use of dynamic SIMS and strict cryogenic sample treatment Chandra et al. managed

*Corresponding author: Professor Håkan Nygren, Department of Anatomy and Cell Biology, Göteborg University, PO Box 420, SE 405 30 Göteborg, Sweden. E-mail: hakan.nygren@anatcell.gu.se.

to visualize ^{39}K, ^{23}Na and ^{40}Ca levels in a LLC-PK cell line [1] and more recently isotopically labeled molecules, for example ^{14}C and ^{129}I [5]. The ion images displayed a normal cellular ion distribution and could therefore be used for identification of individual cells and especially cells with ruptured cell membranes. The system did however not allow direct identification of other, larger molecular species.

Colliver and colleagues [3] utilised a freeze-fracture system located within an ultra-high vacuum environment and TOF-SIMS to image cocaine exposed bacteria and achieved micrometer resolution images of inorganic ions. More recently, in the same group, Pacholski and colleagues [9] developed the biological imaging technique further and were able to image the phosphocholine headgroup 184 Da in freeze-fractured, frozen-hydrated phosphatidylcholine dipalmitoyl liposomes and cholesterol 386 Da in phosphatidyl-n-monomethyl ethanolamine dipalmitoyl/cholesterol liposomes. To some extent were they also able to image a choline fragment, 86 Da, in freeze-fractured, frozen-hydrated red blood cells. Roddy et al. [10] developed their work further and used the same methods to study freeze-fractured PC12 cells. Again they managed, to some extent, to create ion images of the phosphocholine headgroup, 184 Da, resembling the known cellular structure of the PC12 cells. Attempts to image cholesterol showed only limited spatial correlation, between the ion images and the known cell structures.

We here report successful subcellular localisation of membrane lipids by pattern recognition imaging TOF-SIMS (PRITS) based on freeze-drying thin layers of cells in volatile salt solutions, combined with imprinting the cell layer onto a silver foil.

2. Materials and methods

2.1. Cell preparation

Capillary blood from healthy donors was placed in drops on a clean glass surface (microscope slide) and incubated for 30 min at 37°C. The clot was rinsed off with Dulbeccos phosphate-buffered saline (D-PBS), leaving a monolayer of glass-adhering polymorphonuclear leukocytes (PMNLs) and a few platelets as shown previously [11] and verified here by fluorescence- and scanning electron microscopy (SEM).

Freeze drying was performed as described by Warley et al. [12]. Briefly, the D-PBS was removed from the glass adhering cells by a rinse in 0.15M NH4COOH at pH 7.2–7.4. The glasses were then placed on a solid copper block, precooled with liquid nitrogen, in a vacuum chamber that was evacuated down to 10^{-4}–10^{-5} bar over night. The samples were then stored in a desiccated chamber at room temperature for up to 4 h prior to TOF-SIMS analysis.

2.2. Silver imprint

Imprints of the dry cells were made by pressing a clean silver foil against the glass surfaces with deposited cells. The imprinting technique has been described previously by Sjövall et al. (submitted for publication in *Analytical Chemistry*). This procedure cuts the freeze-dried cell into two parts and transfers cell nuclei and membrane to the silver foil, as seen in Fig. 1. The silver foil (99.98%, thickness 0.1 mm, Goodfellow, UK) was cleaned and etched in HNO_3 immediately before making the cell imprint. Pure silver foil was used as background control in all measurements. Cholesterol (99+%, Sigma, St Lois, MO, USA) and phosphatidylcholine type XVI-E (approx. 99%, Sigma, St Lois, MO, USA) was dissolved in chloroform and applied on silver foil, as standards for cholesterol and phosphocholine identification.

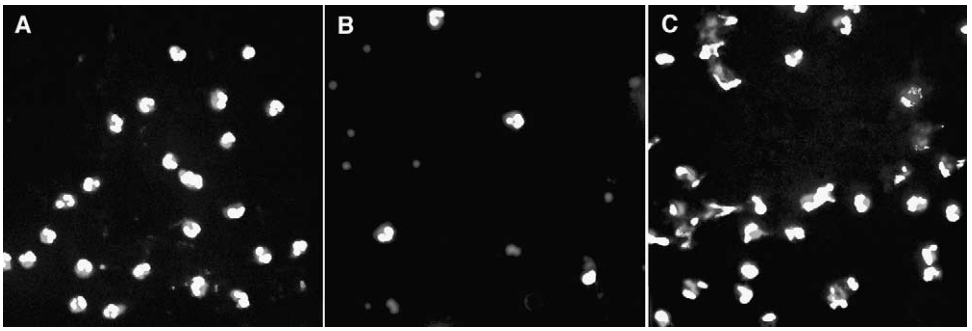

Fig. 1. Fluorescence micrograph study of PMNL cell imprinting. Fluorescence micrographs showing the distribution of DNA (Hoechst 33342 staining) and F-actin (phalloidin staining) of freeze-dried PMNL cells on the glass substrates. The Hoechst 33342 stain is seen as an intense white colour in the central areas of the cells and the phalloidin staining as a grayscale surrounding the nucleus. A, shows the glass surface before imprinting, B, the glass surface after imprinting and C, the silver imprint.

2.3. Fluorescence microscopy

The glass slides and pieces of silver foil were double-stained with FITC-conjugated Phalloidin (Sigma, St Louis, MO, USA) and Hoechst 33342 (Sigma, St Louis, MO, USA) to further examine the imprinting quality. The specimens were first stained with FITC-conjugated Phalloidin (40 minutes, 50 mg/ml), to detect actin filaments. After staining the specimens were rinsed in D-PBS and then stained with Hoechst 33342 (3 minutes, 20 μg/ml), to visualize cell nuclei. After a final rinse in D-PBS the samples were mounted in 1,4-diaza-bicyclo[2,2,2]octane (DABCO) to keep the fluorescence from fading. The specimens were stored at 6°C until further examination.

The specimens were examined and photographed in an Axioskop 2 Plus fluorescence microscope (Zeiss, Germany) equipped with a CCD camera (SPOT 2, Diagnostic instruments Inc., USA). Fluorescence images of cells adhering to glass, before and after imprinting, as well as of the imprint on silver foil are shown in Fig. 1.

2.4. Scanning electron microscopy

To verify the effects of the freeze-drying process, the specimens were examined and photographed in a JEOL JSM-5800 scanning electron microscope (SEM) fitted with a Link ISIS energy dispersive X-ray system. Before examinations the specimens were sputter-coated with a gold–palladium coating. The SEM was operated in the secondary electron imaging mode at acceleration voltages between 3 and 15 kilovolts depending on the properties of the different samples. The smallest objective lens aperture of the instrument was used and the beam current was kept as low as possible in order to minimize specimen damage without getting too poor signal-to-noise ratio. The working distance was kept to 10 millimetres in all the SEM examinations. Figure 2 shows a freeze-dried PMN leukocyte adhering to the glass surface.

2.5. Mass spectrometry

The cell-imprinted Ag surfaces were analysed on a TOF-SIMS IV instrument (Ion-ToF GmbH) using a pulsed primary beam of focussed 25 keV Ga^+ ions. High resolution TOF-SIMS images (lateral resolution1 μm) and spectra ($m/\Delta m = 7000$–8000) were recorded separately. The analysis area was normally

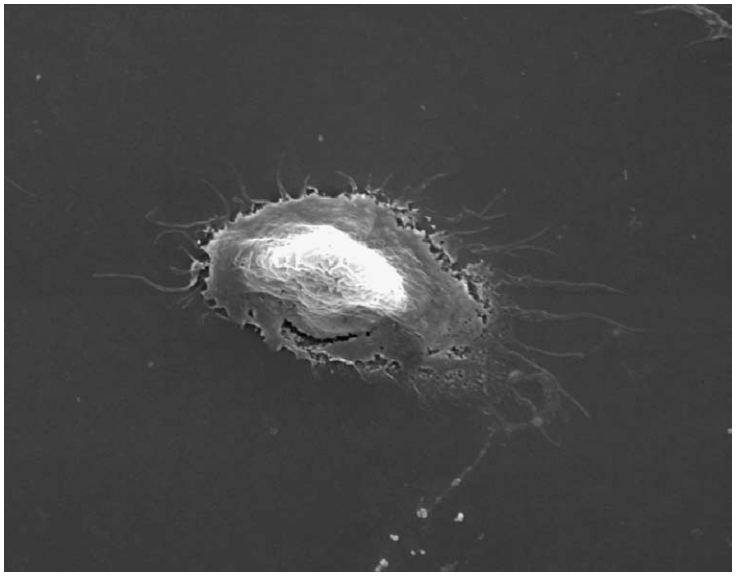

Fig. 2. Scanning electron micrograph of a freeze-dried PMN leukocyte. A scanning electron micrograph of a freeze-dried glass-adhering polymorphonuclear leukocyte(PMNLs) at 3500× magnification.

$100 \times 100\ \mu m^2$ and the primary ion beam current was 0.5 pA (analysis time 100 s) and 1.0 pA (analysis time 70 s) in the high mass resolution and high lateral resolution modes, respectively.

A TOF-SIMS spectrum is recorded by scanning the primary ion beam over the analysis area and acquiring a mass spectrum of positive or negative ions leaving the surface. The accumulated primary ion dose was kept below the so called static limit (10^{13} electrons/cm^2) [13], which means that the analysis is completed before the organic compounds in analysed area have been significantly damaged by the primary ions. In a TOF-SIMS image, the brightness of each pixel reflects the signal intensity of a selected ion in that pixel, thereby visualizing the lateral distribution of the selected compound within the analysis area. The recorded TOF-SIMS spectra were stored in raw data files which contain complete spatial and spectral information from the data collection, thereby allowing for subsequent extraction of images of arbitrary ions as well as extraction of mass spectra from restricted areas within the analysis area at any time after data collection.

3. Results

The SEM micrographs of the surface adhering PMNLs, exemplified in Fig. 2, show that the freeze-dried cells appear normal and retain their characteristic structure. Therefore the information from the fluorescence images, in Fig. 1, show what can be transferred to the silver imprints and analysed by TOF-SIMS. The cell nuclei, stained with Hoechst 33342, appear as bright white in the images, whereas actin filaments, stained with Phalloidin, are shown in greyscale. Figure 1A, shows the glass surface before imprinting, Fig. 1B, the glass surface after imprinting and Fig. 1C, the silver imprint. The fluorescence image of the silver imprint show that both cell nuclei and plasma membrane are transferred to the silver surface.

The reference spectra of pure cholesterol and phosphatidylcholine, deposited as monolayers, on silver foil, are shown in Fig. 3.

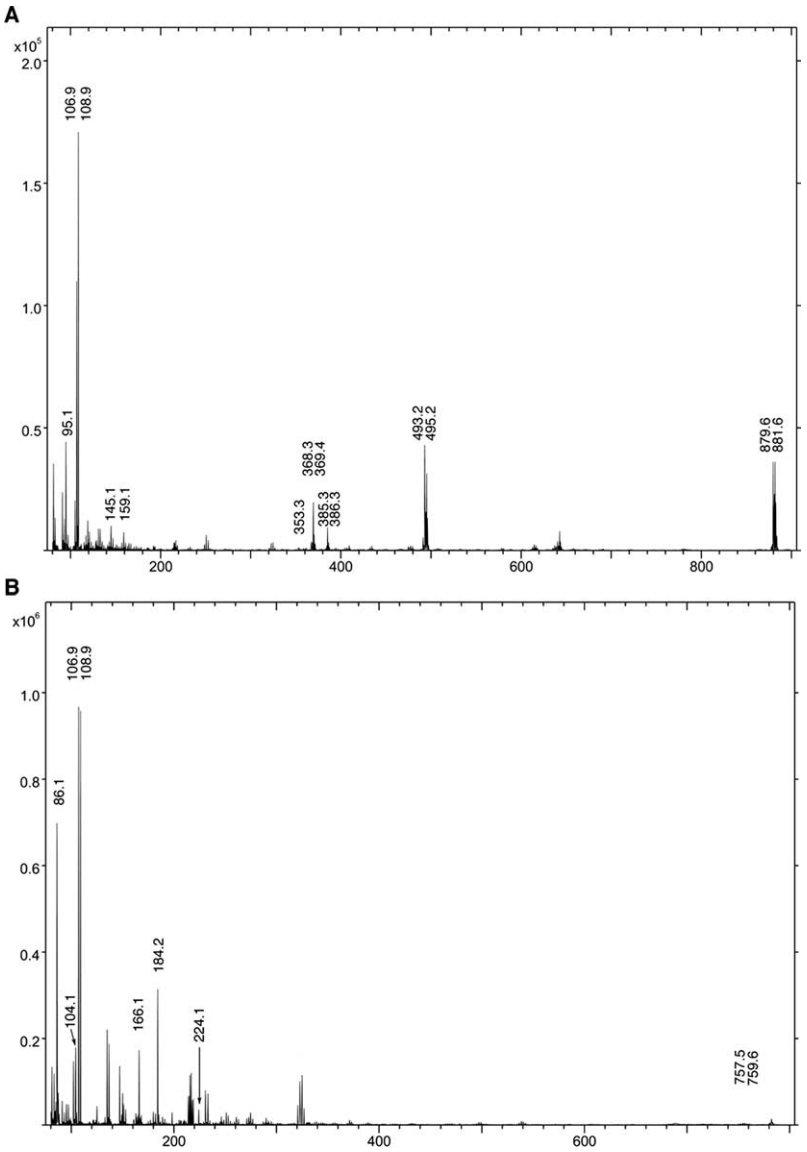

Fig. 3. TOF-SIMS reference spectra. Figure 3A: cholesterol reference spectrum. A TOF-SIMS cholesterol reference spectrum obtained at a maximum resolution of $m/\Delta m = 7000$ on a silver surface. The peaks at 493.2 and 495.2 represents the silver cationised cholesterol molecular ion $[M+^{107}Ag]^+$ and $[M+^{107}Ag]^+$. The 879.6 and 881.6 peaks represents the silver cationised cholesterol dimer $[2M+^{107}Ag]^+$ and $[2M+^{109}Ag]^+$. Cholesterol fragment peak can be seen at 386.3 Da, 385.3 Da, 369.4 Da, 368.3 Da, 353.3 Da, 159.1 Da, 145.1 Da and 95.1 Da. Furthermore two peaks at 106.9 and 108.9, representing $^{107}Ag^+$ and $^{109}Ag^+$, can be seen. Other visible non-labelled peaks are silver ion complexes or unidentified peaks. Figure 3B: phosphatidylcholine reference spectrum. A TOF-SIMS phosphatidylcholine reference spectrum obtained at a maximum resolution of $m/\Delta m = 7000$ on a silver surface. Peaks representing 16 : 0/18 : 2 and 16 : 0/18 : 1 phosphatidylcholine can be seen at 757.5 and 759.6. Only one species of silver cationised phosphatidylcholine molecular ion could be located but with very low intensity (not shown). Yet several phosphocholine derived peaks is visible at 224.1 Da, 184.2 Da, 166.1 Da, 104.1 and 86.1 Da. Furthermore two peaks at 106. 9 and 108.9, representing $^{107}Ag^+$ and $^{109}Ag^+$, can be seen. Other visible non-labelled peaks are silver ion complexes or unidentified peaks.

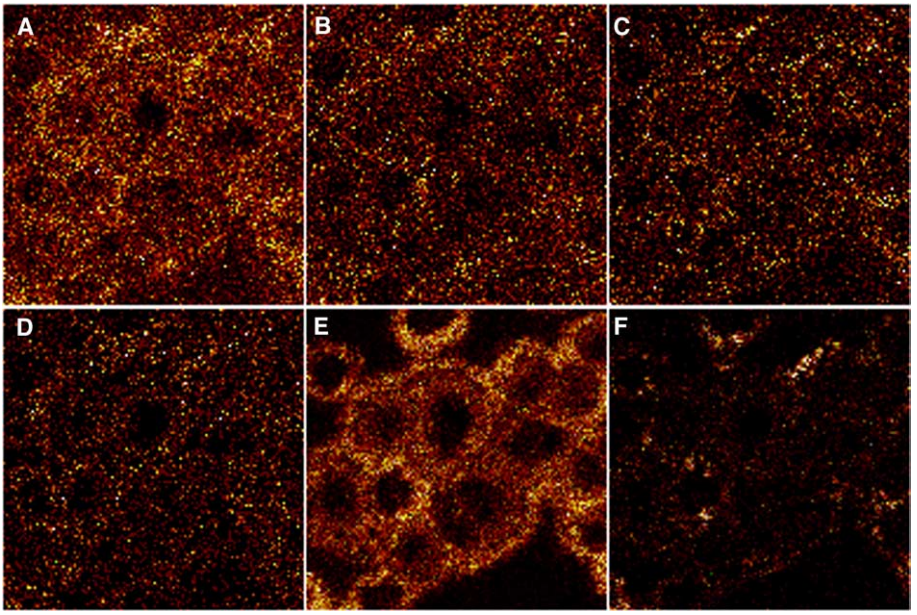

Fig. 4. TOF-SIMS cholesterol ion images of freeze-dried fractured PMN cells. TOF-SIMS ion images of freeze-dried fractured PMN cells imprinted on a silver surface, displaying ions with a total count over 5000 and masses above 90 Da, at a field of view of 100.6 × 100.6 μm^2. The primary ion beam current was 0.5 pA and the analysis time 70 s. A, represents the ion image of $[C_7H_{11}]^+$ at 95 Da, with a total count of 30407. B, represents the ion image of $[C_{11}H_{13}]^+$ at 145 Da, with a total count of 11845. C, represents the ion image of $[C_{12}H_{15}]^+$ at 159 Da, with a total count of 7077. D, represents the ion image of the $[M–OH]^+$ cholesterol fragment at 369 Da with a total count of 5596. E, represents the merged ion images of the silver bound cholesterol molecular ions $[M+^{107}Ag]^+$ and $[M+^{109}Ag]^+$, at 493 Da and 495 Da. F, represents the merged in images of the silver bound cholesterol dimer $[2M+^{107}Ag]^+$ and $[2M+^{109}Ag]^+$, at 880 Da and 882 Da, respectively.

In accordance with previous work by Seedorf and others [14] the major cholesterol-derived peaks in the reference cholesterol sample were seen at 493.2 Da $[M+^{107}Ag]^+$ and 495.2 Da $[M+^{109}Ag]^+$. Further more, we detected peaks representing a cholesterol dimer at 879.6 Da $[2M+^{107}Ag]^+$ and 881.6 Da $[M+^{109}Ag]^+$. Minor peaks were detected at 386.3 Da $[M]^+$, 385.3 Da $[M–H]^+$, 369.4 Da $[M–OH]^+$, 368.3 Da $[M–H_2O]^+$ and 353.3 Da $[M–CH_3H_2O]^+$. Other minor fragment peaks were found at 159.1 Da, 145.1 Da and 95.11 Da with suggested identification as $[C_{12}H_{15}]^+$, $[C_{11}H_{13}]^+$ and $[C_7H_{11}]^+$, respectively.

In the phosphatidylcholine spectra, several peaks representing previously known [9] fragments of phosphatidylcholine could be identified. The major peaks represent the phosphocholine headgroup $[C_5H_{15}PNO_4]^+$ at 184.1 Da, choline $[C_5H_{14}NO]^+$ at 104.1 Da and a choline fragment $[C_5H_{12}N]^+$ at 86.1 Da. A weaker fragment $[C_5H_{13}PNO_3]^+$ at 166.1 Da representing the phosphocholine headgroup with the loss of H_2O could also be found as well as a fragment at $[C_8H_{17}PNO_5]^+$ 224.1 Da, probably representing phosphocholine and the glycerol backbone of the parent molecule. A few peaks representing the molecular ions of phosphatidylcholine could be identified. Yet only phosphatidylcholine with fatty acid chain lengths of 16 : 0/18 : 2 and 16 : 0/18 : 1, at 757.5 Da and 759.6 Da, could be identified as to be unique for the phosphatidylcholine reference spectra. A silver cationised quasimolecular ion of 16 : 0/18 : 1 phosphatidylcholine could be detected in the reference spectra, but with a low intensity.

When applying the reference cholesterol data to the freeze-dried cell samples we were able to achieve molecular imaging of all major ions detected in he cholesterol reference sample, as seen in Fig. 4. The

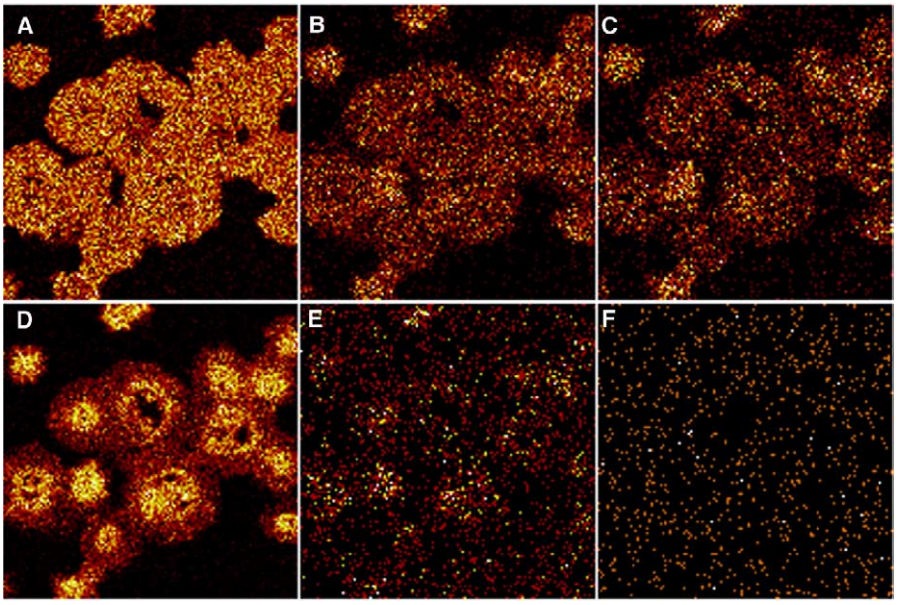

Fig. 5. TOF-SIMS phosphatidylcholine ion images of freeze-dried fractured PMN cells. TOF-SIMS ion images of freeze-dried fractured PMN cells imprinted on a silver surface, displaying ions with a total count over 1000 and masses above 80 Da, at a field of view of 100.6 × 100.6 μm^2. The primary ion beam current was 2.2 pA and the analysis time 70 s. A, represents the ion image of a choline fragment $[C_5H_{12}N]^+$ at 86 Da with a total count of 50029. B, represents choline $[C_5H_{14}NO]^+$ at 104 Da with a total count of 15554. C, represents the phosphocholine headgroup minus H_2O, $[C_5H_{13}PNO_3]^+$ at 166 Da with a total count of 8744. D, represents the phosphocholine ion $[C_5H_{15}PNO_4]^+$ at 184 Da with a total count of 46947. E, represents the fragment ion $[C_8H_{17}PNO_5]^+$ at 224 Da with a total count of 3180. F, represents the parent 16 : 0/18 : 2 phosphatidylcholine ion at 758 with a total count of 1016.

molecular cholesterol ions, $[M+^{107}Ag]^+$ and $[M+^{109}Ag]^+$, dominated the images with a total count of more than 40000. The dimer cholesterol ions, $[2M+^{107}Ag]^+$ and $[2M+^{109}Ag]^+$, could be shown with a total count of more than 30000. The ions, 369.4 Da $[M–OH]^+$, 159.1 Da $[C_{12}H_{15}]^+$, 145.1 Da $[C_{11}H_{13}]^+$ and 95.11 Da $[C_7H_{11}]^+$ had total counts ranging between 5000 and 30000 and could therefore be imaged with good contrast.

In the molecular images, there was a high spatial correlation between the different cholesterol fragment ions and the molecular cholesterol ions, $[M+^{107}Ag]^+$ and $[M+^{109}Ag]^+$. The ion images of the ions, $[2M+^{107}Ag]^+$, $[2M+^{109}Ag]^+$, $[M–OH]^+$, 159.1 Da $[C_{12}H_{15}]^+$, 145.1 Da $[C_{11}H_{13}]^+$ and 95.11 Da $[C_7H_{11}]^+$, show qualitatively similar patterns to the ion images of the parent cholesterol ions. Ions with a total count below 5000 resembled the $[M+^{107}Ag]^+$ and $[M+^{109}Ag]^+$ ion images spatially but did not exhibit any significant intensity correlation.

With information of the ion formation from the phosphatidylcholine reference spectra, molecular imaging could be achieved for phosphatidylcholine fragments as well, as seen in Fig. 5. The phosphatidylcholine derived fragment ions $[C_5H_{15}PNO_4]^+$ at 184 Da, $[C_5H_{13}PNO_3]^+$ at 166 Da, $[C_5H_{14}NO]^+$ at 104 Da and $[C_5H_{12}N]^+$ at 86 Da had high total counts, ranging between 8700 and 50000, and could be imaged with good contrast. The ion $[C_8H_{17}PNO_5]^+$ at 224 Da had a lower total count, at about 3000 units, but its localisation showed a good correlation to that of the other phosphatidylcholine ions. Ions corresponding to the various species of phosphatidylcholine parent ions could not be imaged with good contrast, due to their relatively low countrate. Therefore imaging of phosphatidylcholine distribution could not be established specifically, rather a more general phosphocholine distribution is

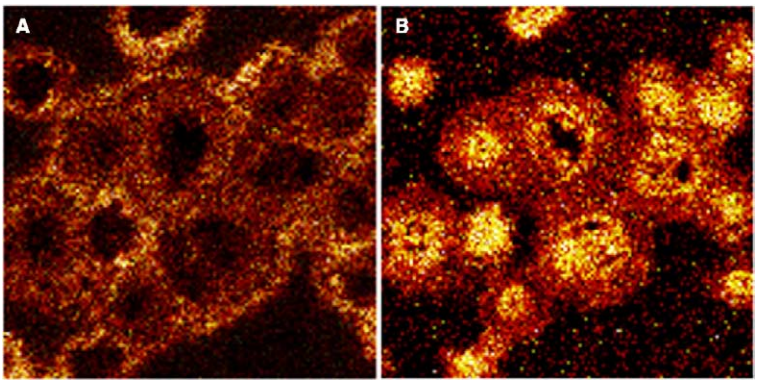

Fig. 6. Combined TOF-SIMS ion images. A: combined images from cholesterol. The collection of separate ion images, $[2M+^{107}Ag]^+$, $[2M+^{109}Ag]^+$, $[M–OH]^+$, 159.1 Da $[C_{12}H_{15}]^+$, 131.1 Da $[C_{10}H_{11}]^+$ and 95.11 Da $[C_7H_{11}]$, into one image of the cholesterol distribution in surface-adhering PMNLs at a field of view of 100.6 × 100.6 μm^2. B: combined images from phosphocholine. The collection of separate ion images of the phosphocholine fragments, $[C_5H_{15}PNO_4]^+$ at 184 Da, $[C_5H_{13}PNO_2]^+$ at 166 Da and $[C_8H_{17}PNO_5]^+$ 224 Da, into one image at a field of view of 100.6 × 100.6 μm^2. The phosphocholine fragment ion images show a distribution localized to the central areas of the cells.

displayed in the ion images. All phosphocholine containing lipid species, such as sphingomyelin and platelet activating factor, will therefore contribute to the images. The different phosphocholine fragment ion images differed slightly in localisation and intensity. This may be due to differences in fragment ion intensity between the different phosphocholine containing lipids and to contributions from adjacent ions in the spectra, not being resolved due to the low mass-resolution nature of the high spatial-resolution images obtained. The high lateral resolution of the images, limits the mass resolution to $m/\Delta m = 800$–1000, compared to $m/\Delta m = 8000$ for the high mass resolution spectra. The imaged ions $[C_5H_{14}NO]^+$ at 104 Da and $[C_5H_{12}N]^+$ at 86 Da have adjacent ions ion the high-mass resolution spectra that could contribute to the ion images obtained. The other ions detected in the phosphatidylcholine spectra did not have adjacent peaks that could contribute to the ion images.

The collection of separate peaks, $[2M+^{107}Ag]^+$, $[2M+^{109}Ag]^+$, $[M–OH]^+$, 159.1 Da $[C_{12}H_{15}]^+$, 145.1 Da $[C_{11}H_{13}]^+$ and 95.11 Da $[C_7H_{11}]^+$, into one image (PRITS) of the cholesterol distribution in surface-adhering PMNLs is shown in Fig. 6A. The obtained images show a distribution of the cholesterol derived ions, that seem to be primarily located to what could be interpreted as the outer rim of the cells, i.e. localized to the plasma membrane, a distribution that matches the previously known distribution of cellular cholesterol [15]. A patchy distribution of cholesterol could be seen, and the patches are apparently formed by smaller spherical 1–2 μm diameter cholesterol-rich spots.

Figure 6B shows the distribution of phosphocholine fragments from the collection of 3 separate peaks detected in the phosphatidylcholine spectra, $[C_5H_{15}PNO_4]^+$ at 184 Da, $[C_5H_{13}PNO_2]^+$ at 166 and $[C_8H_{17}PNO_5]^+$ 224, into one image. The phosphocholine fragment ion image shows a signal distribution localized to the central areas of the cells. This distribution is probably due to contribution from the nuclear membranes, since granular ER and nuclear membranes contain approximately 70% phosphatidylcholine [16].

4. Discussion

PRITS, the imaging of several fragment ions from a substance and analysis of the localisation of the imaged fragments presents a suitable approach to the study of different substances in freeze-dried cells.

For cholesterol and phosphocholine, the imaging of several fragment ions from each substance and the mutual co-localisation of these fragments present a probable representation of the actual localisation of that particular substance in the freeze-dried cells. The complementary nature of the cholesterol and the phosphocholine ion images support this view, since such a complementary relation is well known to exist [15,16]. To use several fragment ions from each substance for imaging is suitable since it allows for a more precise interpretation of the obtained ion images and a greater awareness of possible contributions from other adjacent non-specific ions.

It is well recognized that cell membranes are organized in functional rafts of differential lipid composition [17,18]. Fluorescent probe techniques have been utilized to examine membranes in viable cells, indicating that the rafts may form aggregates of up to a few microns in size [19,20]. The resolution of this technique ($\geqslant$0.5 μm) limits the possibility to study the formation of these aggregates. Studies at the TEM-level have also been performed (20) by using filipin, a polyene antibiotic that binds to cholesterol. Cholesterol-enriched caveolae, 50–80 nm in size, were seen clustered in groups of 5–10 vacuoles. The three-dimensional distribution of these clusters was not studied. The structures seen in Fig. 4 and in Fig. 6A may thus represent clustered caveolae [21], or aggregated rafts [19,20].

5. Conclusion

The PRITS-technique presented here with its resolution approaching 100 nm and large image field may be very useful in further studies of the lateral heterogeneity of the lipid composition of membranes.

References

[1] S. Chandra and G.H. Morrison, *Biol. Cell.* **74** (1992), 31–42.
[2] J. Clerc, C. Fourre and P. Fragu, *Cell. Biol. Int.* **21** (1997), 619–633.
[3] T.L. Colliver, C.L. Brummel, M.L. Pacholski, F.D. Swanek, A.G. Ewing and N. Winograd, *Anal. Chem.* **69** (1997), 2225–2231.
[4] R. Levi-Setti, J.M. Chabala, K. Gavrilov, R. Espinosa, 3rd and M.M. Le Beau, *Microsc. Res. Tech.* **36** (1997), 301–312.
[5] S. Chandra, D.R. Smith and G.H. Morrison, *Anal. Chem.* **72** (2000), 104A–114A.
[6] C.A. McCandlish, J.M. McMahon and P.J. Todd, *J. Am. Soc. Mass Spectrom.* **11** (2000), 191–199.
[7] P.J. Todd, T.G. Schaaff, P. Chaurand and R.M. Caprioli, *J. Mass Spectrom.* **36** (2001), 355–369.
[8] R. Strick, P.L. Strissel, K. Gavrilov and R. Levi-Setti, *J. Cell. Biol.* **155** (2001), 899–910.
[9] M.L. Pacholski, D.M. Cannon, Jr., A.G. Ewing and N. Winograd, *Rapid Commun. Mass Spectrom.* **12** (1998), 1232–1235.
[10] T.P. Roddy, D.M. Cannon, Jr., C.A. Meserole, N. Winograd and A.G. Ewing, *Anal. Chem.* **74** (2002), 4011–4019.
[11] N. Yahyapour and H. Nygren, *Colloids Surf. B Biointerfaces* **15** (1999), 127–138.
[12] A. Warley and J.N. Skepper, *J. Microsc.* **198**(Pt 2) (2000), 116–123.
[13] J.C. Vickerman. in: *ToF-SIMS: Surface Analysis by Mass Spectrometry*, J.C. Vickerman and D. Briggs, eds, IM Publications and SurfaceSpectra Limited, West Sussex, Manchester 2001, pp. 1–40.
[14] U. Seedorf, M. Fobker, R. Voss, K. Meyer, F. Kannenberg, D. Meschede, K. Ullrich, J. Horst, A. Benninghoven and G. Assmann, *Clin. Chem.* **41** (1995), 548–552.
[15] Y. Lange, M.H. Swaisgood, B.V. Ramos and T.L. Steck, *J. Biol. Chem.* **264** (1989), 3786–3793.
[16] J.M. Boon and B.D. Smith, *Med. Res. Rev.* **22** (2002), 251–281.
[17] K. Simons and E. Ikonen, *Nature* **387** (1997), 569–572.
[18] L. Liscum and N.J. Munn, *Biochim. Biophys. Acta* **1438** (1999), 19–37.
[19] A.V. Samsonov, I. Mihalyov and F.S. Cohen, *Biophys. J.* **81** (2001), 1486–1500.
[20] K. Gousset, W.F. Wolkers, N.M. Tsvetkova, A.E. Oliver, C.L. Field, N.J. Walker, J.H. Crowe and F. Tablin, *J. Cell. Physiol.* **190** (2002), 117–128.
[21] J. Thyberg, *J. Histochem. Cytochem.* **50** (2002), 185–195.